ChemComm

COMMUNICATION

View Article Online
View Journal | View Issue

Cite this: *Chem. Commun.*, 2014, 50, 4434

Received 31st January 2014,
Accepted 4th March 2014

DOI: 10.1039/c4cc00857j

www.rsc.org/chemcomm

Oxygen and methanol mediated irreversible coordination polymer structural transformation from a 3D Cu(I)-framework to a 1D Cu(II)-chain†

Jing-Yuan Ge, Jian-Cheng Wang, Jun-Yan Cheng, Peng Wang, Jian-Ping Ma, Qi-Kui Liu and Yu-Bin Dong*

An interesting irreversible structural transformation visible to the naked-eye occurs when a 3D Cu(I)–polymeric complex $Cu_2L(NO_3)_2(DMF)_{0.4}$ (1) is suspended in CH_3OH in air to produce a 1D-Cu(II) polymeric complex $Cu(\mu\text{-}OCH_3)(L)(NO_3)$ (2) (L = 1,2-bis[4-(pyrimidin-4-yl)phenoxy]ethane). The transformation mechanism from 1 to 2 was also investigated.

In coordination polymers,[1] structural transformation,[2] which is caused by some external stimuli such as solvent, ionic templates and ligand exchange,[3] light,[4] temperature variation[5] and sometimes mechanochemical forces,[6] often occurs. In some cases, structural transformations based on the coordination polymers are accompanied with the dimensionality and color changes resulting from the variation of the central metal valence and metal coordination mode. Such a stimuli-responsive dynamic structural transformation is important, which is very useful in the preparation of new switching or sensing materials.

Among the various metal-complexes structural transformations, the transformation of copper species is more interesting and valuable. As we know, copper proteins in biological systems can provide various functions including dioxygen transport by hemocyanin, oxygenation and dehydrogenation of substrates combined with the transformation of O_2 to either H_2O_2 or water.[7] For understanding and mimicking such biological oxygenation behaviors, the synthesis of new Cu(I)-coordinating systems and the investigation of their spontaneous oxygenation are necessary. Such effort will generate a sufficiently large database from which the specific artificial bionic enzymes could be sieved out.

Our previous studies showed that the coordination polymers generated from open-chain polyether-bridged organic linkers are flexible. For example, the polymeric coordination patterns could be tuned by the temperature based on the ligand conformation variation.[8] Motivated by our interest in temperature-dependent synthesis of coordination polymers, in this contribution, we report two new coordination polymers $Cu_2(\mathbf{L})(NO_3)_2(DMF)_{0.4}$ (**1**, orange) and $Cu(\mu\text{-}OCH_3)(\mathbf{L})(NO_3)$ (**2**, green-blue) based on a new open-chain polyether-bridged organic spacer **L** at different temperatures (Scheme S1, ESI†). The flexible ligand **L** respectively adopts *trans*- and *cis*-conformations at high (90 °C) and low temperatures (r.t.), which is in good agreement with our previous observation.[8] Notably, **1** undergoes an oxygen and methanol triggered structural transformation to **2**, visible to the naked-eye and the structural feature changed from a 3D porous framework (**1**) to a 1D double chain motif (**2**), and the valence of the copper ion changed from univalent to bivalent correspondingly. The dioxygen was supposedly transformed to H_2O_2 *via* the superoxide radical anion during the structural transformation process.

As shown in Scheme 1, compound **1** was isolated as an orange crystalline solid by the combination of **L** (molar ratio **L** : Cu(II) = 1 : 2) in a mixed-solvent system (DMF/MeCN) at 90 °C in good yield (65%).

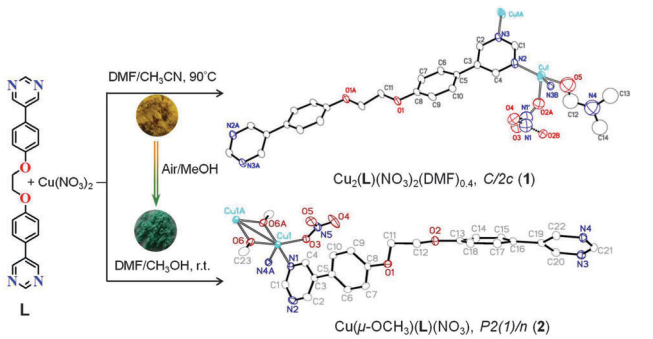

Scheme 1 Representation of the synthesis of **1–2** and the structural transformation from **1** to **2**. Crystals of **1**, on being kept in MeOH in the air at the ambient temperature for about 36 h, undergo a visual irreversible structural transformation to yield a green-blue product **2** (the color change is shown in the figure with powdered samples of **1** and **2**).

College of Chemistry, Chemical Engineering and Materials Science, Collaborative Innovation Center of Functionalized Probes for Chemical Imaging, Key Laboratory of Molecular and Nano Probes, Ministry of Education, Shandong Normal University, Jinan 250014, P. R. China.
E-mail: yubindong@sdnu.edu.cn

† Electronic supplementary information (ESI) available: Synthesis and characterization data for all compounds, including figures for ORTEP, XPS, XRPD, ^{1}H NMR, IR, CIF files and crystal data. CCDC 984134 and 984135. For ESI and crystallographic data in CIF or other electronic format see DOI: 10.1039/c4cc00857j

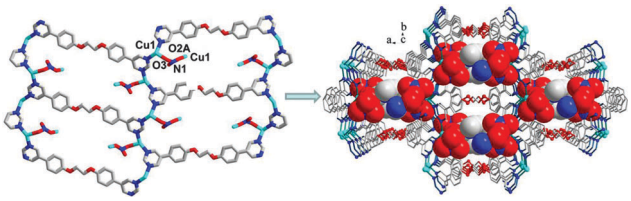

Fig. 1 The Cu(I) nodes in **1** are connected to each other by the tetradentate **L** into a 2D net. These 2D nets are further interlocked together through μ-NO_3^- (Cu(1)–O(3)–N(1)–O(2)–Cu(1) linkage, basically perpendicular to the net plane) into a 3D framework containing square-like channels, in which the disordered DMF and NO_3^- are located. The disordered DMF molecules are omitted for clarity in left figure, and the DMF and NO_3^- in right figure are shown in space-filling model.

Single-crystal analysis (ESI†) revealed that compound **1** crystallizes in the monoclinic *C*2/*c* space group.

As shown in Fig. 1, each Cu(I) center in **1** lies in a tetrahedral $\{CuN_2O_2\}$ coordination sphere. The two N-donors come from two terminal pyrimidyl groups and two O-donors come from a coordinated NO_3^- anion and a coordinated DMF solvent molecule, respectively. In the solid state, Cu(I) nodes are linked together by the *trans*-tetradentate **L** linkers into a 2D net extended in the crystallographic *ab* plane (Fig. 1). These 2D nets are further interlocked together by the μ-NO_3^- to form a 3D framework containing square-like open channels (dimensions ~ 10 × 10 Å) running along the crystallographic *c* axis. The shortest interlayer Cu(I)···Cu(I) distance is 5.440 Å. The disordered NO_3^- anions and DMF molecules are located in the channels (Fig. 1). XRPD patterns indicated that the obtained sample is pure, and the X-ray photoelectron spectroscopy (XPS) measurements indicate that the copper center in **1** is univalent (Fig. 2),[9] which is well in agreement with the single-crystal X-ray diffraction analysis (ESI†).

Compound **2** was obtained as a green-blue crystalline solid in a DMF–MeOH mixed-solvent system at room temperature. It is different from **1**, the ligand **L** in **2** adopts *cis*-conformation, and as a bidentate linker to bind copper nodes. Single-crystal X-ray diffraction studies (ESI†) revealed that **2** crystallizes in the monoclinic space group *P*2(1)/*n*. Each Cu(II) node locates in a square pyramidal coordination sphere $\{CuN_2O_3\}$, which is composed of two pyrimidyl N-donors (d_{Cu-N} bond lengths are 2.024(3) and 2.333(3) Å, respectively), three O atoms from one monodentate nitrate (d_{Cu-O} = 2.160(11) Å) and two bridging methoxide groups (Cu–O bond lengths range from 1.934(2) to 2.030(2) Å) (Scheme 1). The methoxide groups are co-bridging two Cu(II) nodes to form a $\{Cu_2(\mu\text{-}OCH_3)_2\}$ cluster core. The d_{Cu-Cu} in $\{Cu_2(\mu\text{-}OCH_3)_2\}$ unit is 3.0359(10) Å, while the <Cu–O–Cu angles vary from 76.73(8) to 103.26(2)°. These geometric

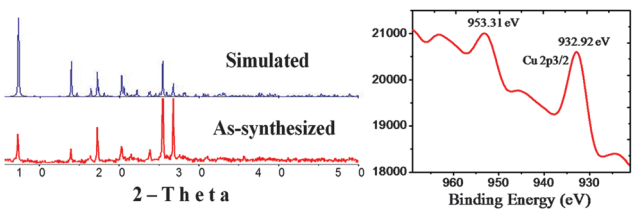

Fig. 2 XRPD pattern (left) and XPS spectrum (right) of **1**.

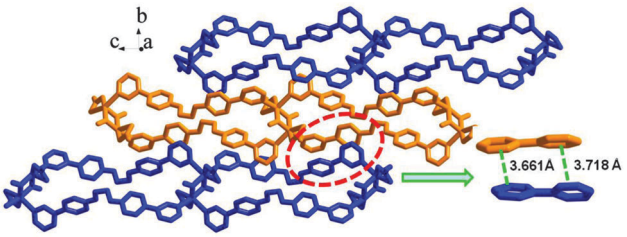

Fig. 3 1D chain of **2** composed of $\{Cu_2(\mu\text{-}OCH_3)_2\}$ cluster cores and **L** in the solid state. The interchain π–π interactions exist in **2**.

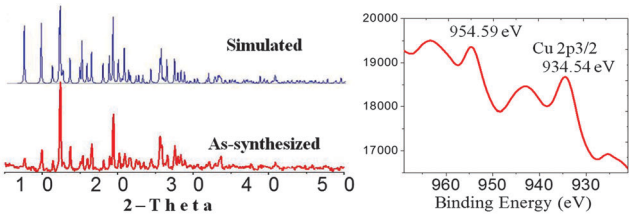

Fig. 4 XRPD pattern (left) and XPS spectrum (right) of **2**.

details are comparable with other reported methoxide-bridged dinuclear Cu(II) compounds.[10] These $\{Cu_2(\mu\text{-}OCH_3)_2\}$ cluster cores are bridged by the *cis*-bidentate ligand **L** into an infinite 1D double chain along the crystallographic *c* axis (Fig. 3). The interchain π–π interactions drive the 1D chains into a 2D net in the crystallographic *bc* plane. Again, the XRPD pattern indicates that the as-synthesized compound **2** is pure (Fig. 4). It is different from **1**, XPS (Fig. 4) and electron paramagnetic resonance (EPR) measurements (Fig. S3, ESI†) of **2** demonstrate that the copper cation is bivalent.[9]

The spontaneous structural transformation from **1** to **2** was accidentally discovered when we explored the solvent-exchange (DMF by MeOH) based on **1** under ambient conditions. The transformation started once compound **1** was suspended in MeOH in air along with a visual color change. As shown in Fig. 5, the color of **1** changed gradually from orange to green-blue (**2**) during the transformation process. Besides the color change visible to the naked eye, the structural transformation process was monitored

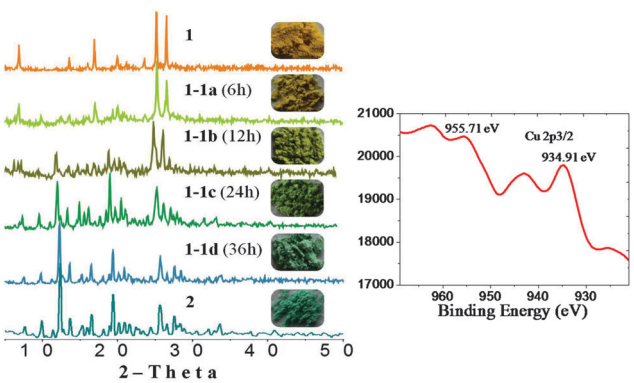

Fig. 5 Left: XRPD patterns of **1**, **1-1a** (in CH_3OH 6 h), **1-1b** (in CH_3OH 12 h), **1-1c** (in CH_3OH 24 h), **1-1d** (in CH_3OH 36 h) and **2**. Photographs showing the color change of the samples of **1** in CH_3OH in air at different time. Right: XPS spectrum of **1-1d**.

by X-ray powder diffraction. As shown in Fig. 5, XRPD patterns show that the peaks corresponding to **2** gradually appeared while the characteristic peaks of **1** disappeared by degrees as time went on. In 36 h, the XRPD pattern of **1-1d** is fully coincident to that of **2**, indicating the structural transformation was finished (from *C*2/*c* to *P*2(1)/*n*). In addition, the IR spectrum performed on **1-1d** shows that the band associated with >C=O at 1655 cm^{-1} has disappeared, indicating that the coordinated DMF molecules are out of the copper coordination sphere (Fig. S4, ESI†).

Besides XRPD patterns, the observation of Cu 2p3/2 peak at 934.91 eV in XPS (Fig. 5) of **1-1d** also demonstrated the oxidization from Cu(I) in **1** to Cu(II) in **2**. The binding energy peak shift of 1.99 eV is consistent with the reported difference of binding energy peak between Cu(I) and Cu(II).[9a] Accordingly, the EPR spectrum of **1-1d** is the same as that of **2** (Fig. S3, ESI†). Furthermore, ICP (Inductively Coupled Plasma) measurements (Fig. S5, ESI†) indicate that the amount of copper in **1-1d** increases from 18.1% (calcd 18.2% in **1**) to 12.1%, which is identical to that of **2** (calcd 12.1%). The elemental analysis also indicated that composition of **1-1d** is the same as that of **2** (Table S1, ESI†). In addition, the process of structural transformation can be accelerated with the increase of the reaction temperature (Table S2, ESI†). For example, the transformation from **1** to **2** at 60 °C (26 h) is much faster than that at room temperature (36 h), indicating that this structural transformation is a dynamic controlled process. Unfortunately, the crystals of **1** did not diffract the X-ray beams due to the loss of the single crystallinity during the transformation process.

We assume herein that the oxygen from air acts as the oxidant in the process of structural transformation. To confirm such an assumption, several parallel experiments were carried out. When compound **1** was suspended in CH_3OH under an N_2 atmosphere at room temperature, the corresponding XRPD pattern indicated that no structural transformation occurred and the framework of **1** remained intact (Fig. S6, ESI†). Secondly, the structural transformation in MeOH is much faster under a pure oxygen atmosphere (22 h) than that in air (36 h) (Fig. S6, ESI†). Besides oxygen, the MeOH medium is also essential for this transformation. As mentioned above, the coordinated DMF molecules in **1** are replaced by MeOH in **2**. When **1** was immersed in other kinds of ROH solvents such as EtOH or i-PrOH, no structural transformation was observed based on the XRPD patterns (Fig. S7, ESI†); the coordinated DMF molecules in **1**, however, are partly exchanged by the corresponding ROH solvent molecules. For different ROH solvents, the water template drives compound **1** to an unknown structural motif based on the X-ray powder diffraction (Fig. S8, ESI†). So, CH_3OH might be a unique co-ligand to facilitate the formation of $\{Cu_2O_2\}$ cluster node during this transformation process, whereas EtOH, i-PrOH and H_2O cannot trigger the transformation of **1** into **2**. It is noteworthy that no ligand was detected in the mother liquor based on the ^1H NMR spectrum (Fig. S9, ESI†), indicating that it might be a solid-state structural transformation.

The isolation of a similar bivalent $Cu_2(OMe)_2$ species from the reaction of Cu(I) precursor bearing cyclic and noncyclic ligands with dioxygen has been reported by some other groups,[11] but the formation process is still not understood. The earlier studies suggest that oxygenation of Cu(I) complexes proceed *via* the formation of a Cu(II)-superoxo species generated from the superoxide radical anions.[12] So the ESR spin-trap technique (with 5,5-dimethyl-1-pyrroline N-oxide, DMPO) was used to detect the $O_2^{-\bullet}$ radical species. When DMPO was added to the MeOH solution of **1**, the ESR spectra clearly indicate that the $O_2^{-\bullet}$ was trapped by DMPO based on the six observed characteristic peaks of the DMPO–$O_2^{-\bullet}$ adducts (Fig. 6).[13] Reasonably, no color change was observed once the $O_2^{-\bullet}$ radicals were trapped by DMPO, indicating that structural transformation from **1** to **2** did not occur. When superoxide dismutase SOD (2000 U mL^{-1}) was added to the above solution, the signal intensities of the $O_2^{-\bullet}$ radical species were significantly weakened as time went on, which further confirmed the formation of $O_2^{-\bullet}$ radical species during the process. According to the above observation, a possible mechanism for this structural transformation was suggested. As shown in Fig. 6, the Cu(I) ion in **1** was oxidized to the Cu(II) ion in **2** by O_2 to generate a Cu(II)–($O_2^{-\bullet}$) superoxo species which further linked one more Cu(I) ion to produce a Cu_2O_2 peroxo species.[14] The peroxo intermediate was anticipated to react with two MeOH to generate a binuclear di-μ-methoxocopper(II) complex and release the H_2O_2.[11e,15]

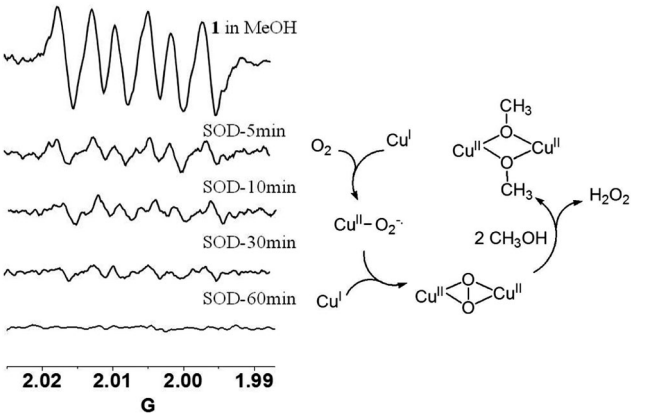

Fig. 6 Left: ESR spectrum of **1** in MeOH with DMPO. The six observed characteristic peaks confirm the formation of the DMPO–$O_2^{-\bullet}$ adducts, and the signal intensity change of ESR spectra after addition of SOD to it. Right: the suggested transformation mechanism.

In summary, we have synthesized two coordination polymers generated from a new ethylene glycol ether-bridged dipyrimidyl ligand. The different reaction conditions resulted in different metal valences and ligand conformations, and consequently, different coordination patterns. In addition, an interesting irreversible structural transformation from a 3D Cu(I) complex (orange) to a 1D Cu(II) chain (green-blue) detectable by the naked eye was observed. The O_2 and CH_3OH medium are the indispensable factors to induce this transformation. The formed $O_2^{-\bullet}$ radical anion, an essential active species for the structural transformation, was trapped by DMPO and SOD, which provided solid evidence for the Cu(I) spontaneous oxygenation in air, and furthermore, a useful O_2 transformation mode based on Cu(I) coordination species.

We are grateful for financial support from the 973 Program (Grant No. 2012CB821705 and 2013CB933800), NSFC (Grant No. 21271120 and 21101099) and "PCSIRT".

Notes and references

1 (*a*) H.-C. Zhou, J. R. Long and O. M. Yaghi, *Chem. Rev.*, 2012, **112**, 673; (*b*) Y. Cui, Y. Yue, G. Qian and B. Chen, *Chem. Rev.*, 2012, **112**, 1126; (*c*) L. E. Kreno, K. Leong, O. K. Farha, M. Allendorf, R. P. V. Duyne and J. T. Hupp, *Chem. Rev.*, 2012, **112**, 1105.
2 J. J. Vittal, *Coord. Chem. Rev.*, 2007, **251**, 1781.
3 (*a*) C.-D. Wu and W. Lin, *Angew. Chem., Int. Ed.*, 2005, **44**, 1958; (*b*) B. Manna, A. K. Chaudhari, B. Joarder, A. Karmakar and S. K. Ghosh, *Angew. Chem., Int. Ed.*, 2013, **52**, 998; (*c*) S. B. Choi, H. Furukawa, H. J. Nam, D.-Y. Jung, Y. H. Jung, A. Walton, D. Book, M. O'Keeffe, O. M. Yaghi and J. Kim, *Angew. Chem., Int. Ed.*, 2012, **51**, 8791; (*d*) H. Long, Y. Tatsu, Z.-H. Lu and Q. Xu, *J. Am. Chem. Soc.*, 2010, **132**, 5568; (*e*) S. Henke, A. Schneemann, A. Wütscher and R. A. Fischer, *J. Am. Chem. Soc.*, 2012, **134**, 9464; (*f*) T. Li, M. T. Kozlowski, E. A. Doud, M. N. Blakely and N. L. Rosi, *J. Am. Chem. Soc.*, 2013, **135**, 11688.
4 P. B. Chatterjee, A. Audhya, S. Bhattacharya, S. M. T. Abtab, K. Bhattacharya and M. Chaudhury, *J. Am. Chem. Soc.*, 2010, **132**, 15842.
5 (*a*) C. Avendano, Z. Zhang, A. Ota, H. Zhao and K. R. Dunbar, *Angew. Chem., Int. Ed.*, 2011, **50**, 6543; (*b*) D. J. Lun, G. I. N. Waterhouse and S. G. Telfer, *J. Am. Chem. Soc.*, 2011, **133**, 5806.
6 (*a*) M. Nagarathinam, A. Chanthapally, S. H. Lapidus, P. W. Stephens and J. J. Vittal, *Chem. Commun.*, 2012, **48**, 2585; (*b*) J. Sun, F. Dai, W. Yuan, W. Bi, X. Zhao, W. Sun and D. Sun, *Angew. Chem., Int. Ed.*, 2011, **50**, 7061.
7 (*a*) E. I. Solomon, U. M. Sundaram and T. E. Machonkin, *Chem. Rev.*, 1996, **96**, 2563; (*b*) J. P. Klinman, *Chem. Rev.*, 1996, **96**, 2541; (*c*) S. Ferguson-Miller and G. T. Babcock, *Chem. Rev.*, 1996, **96**, 2889.
8 Y.-B. Dong, Y.-Y. Jiang, J. Li, J.-P. Ma, F.-L. Liu, B. Tang, R.-Q. Huang and S. R. Batten, *J. Am. Chem. Soc.*, 2007, **129**, 4520.
9 (*a*) B. Balamurugan, B. R. Mehta and S. M. Shivaprasad, *Appl. Phys. Lett.*, 2001, **79**, 3176; (*b*) Y. G. Huang, B. Mu, P. M. Schoenecker, C. G. Carson, J. R. Karra, Y. Cai and K. S. Walton, *Angew. Chem., Int. Ed.*, 2011, **50**, 436.
10 (*a*) G. A. van Albada, M. G. van der Horst, I. Mutikainen, U. Turpeinen and J. Reedijk, *J. Mol. Struct.*, 2011, **995**, 130; (*b*) M. R. A. Al-Mandhary and P. J. Steel, *Eur. J. Inorg. Chem.*, 2004, 329.
11 (*a*) N. Kitajima and Y. Mora-oka, *Chem. Rev.*, 1994, **94**, 737; (*b*) T. N. Sorrell, M. R. Malachowski and D. L. Jameson, *Inorg. Chem.*, 1982, **21**, 3250; (*c*) P. L. Holland, K. R. Rodgers and W. B. Tolman, *Angew. Chem., Int. Ed.*, 1999, **38**, 1139; (*d*) K. D. Karlin, J. Shi, J. C. Hayes, J. W. Mckowm, J. P. Hutchinson and J. Zubieta, *Inorg. Chim. Acta*, 1984, **91**, L3; (*e*) H. Y. Ma, M. Allmendinger, U. Thewalt, A. Lentz, M. Klinga and B. Rieger, *Eur. J. Inorg. Chem.*, 2002, 2857.
12 (*a*) H. Fu, L. Zhang, S. Zhang and Y. Zhu, *J. Phys. Chem. B*, 2006, **110**, 3061; (*b*) C. Chen, W. Zhao, P. Lei, J. Zhao and N. Serpone, *Chem.–Eur. J.*, 2004, **10**, 1956.
13 (*a*) J. Kou, Z. Li, Y. Yuan, H. Zhang, Y. Wang and Z. Zou, *Environ. Sci. Technol.*, 2009, **43**, 2919; (*b*) W. Zhao, C. Chen, X. Li and J. Zhao, *J. Phys. Chem. B*, 2002, **106**, 5022.
14 L. M. Mirica, X. Ottenwaelder and T. D. P. Stack, *Chem. Rev.*, 2004, **104**, 1013.
15 (*a*) N. Kitajima, T. Koda, Y. Iwata and Y. Moro-oka, *J. Am. Chem. Soc.*, 1990, **112**, 8833; (*b*) Z. Tyeklar, P. P. Paul, R. R. Jacodson, A. Farooq, K. D. Karlin and J. Zubieta, *J. Am. Chem. Soc.*, 1989, **111**, 388.